A Study of Water Diffusion into a High-Amylose Starch Blend: The Effect of Moisture Content and Temperature

Melissa A. L. Russo,*,† Ekaterina Strounina,§ Muriel Waret,† Timothy Nicholson,† Rowan Truss,† and Peter J. Halley†,‡

The Centre for High Performance Polymers, Centre for Magnetic Resonance, and Australian Institute for Bioengineering and Nanotechnology, University of Queensland, Brisbane, Australia, 4072

Received August 13, 2006; Revised Manuscript Received September 20, 2006

The effect of moisture content and temperature on water diffusion into a modified high amylose (≤90%) maize thermoplastic starch blend was investigated. Gravimetric and magnetic resonance imaging (MRI) studies were conducted to elucidate the diffusion mechanism and diffusion coefficients for this system. The diffusion coefficient data demonstrated that the rate of water diffusion into this blend was significantly dependent upon temperature and moisture content. Water diffusion was faster at higher temperatures and generally for samples stored at higher relative humidity environments. It was revealed from the gravimetric data that water diffusion into this starch blend was Fickian; however, further analysis of the MRI images found that the water diffusion mechanism was exponentially dependent on the concentration. This result was determined by comparing experimental water concentration profiles to a theoretical model calculated using the implicit Crank−Nicolson finite difference method.

Introduction

Starch-based materials have received considerable interest over the past 20 years due to their fast biodegradability, renewability, and low cost. Despite these key advantages, the development of thermoplastic starch (TPS) materials is limited by their mechanical strength and moisture sensitivity.[1,2] To overcome these challenges, it is possible to blend TPS with other biodegradable polymers to obtain a low cost, biodegradable material with improved overall properties. Studying the ingress of water into TPS polymers is important because it has relevance to the biodegradation, storage, drying, and processing of the material.[3] Water diffusion is often the first process of biodegradation.[4]

When a hydrophilic polymer is immersed in water, water molecules diffuse into the polymer to produce a swollen gel.[5] Dissolution of the polymer is prevented if the bonding between neighboring polymer molecules is strong as a result of cross-linking or hydrogen bonding.[5] Swelling of the polymer continues until the forces due to swelling of the polymer balance the osmotic pressure, driving the solvent into the swollen polymer.[5]

The swelling behavior of rubbery systems can be explained by the theories of rubber elasticity.[6,7,8] Swelling in glassy systems is more complicated than for rubbery systems because the polymer swelling required to accommodate imbibed penetrant from the surface is initially constricted by the internal glassy material.[5] Due to the inability of the glassy core to extend, compressive forces build up in the plane of the sample surface, and initial swelling occurs predominantly perpendicular to the surface, giving a thickness increase without a corresponding increase in the longitudinal dimension.[5] Anisotropic swelling of this type was observed by Dreshel et al.[9] for diffusion of acetone vapor into cellulose nitrate films and by Park et al.[10] for methylene chloride diffusion into polystyrene.

Relaxation of the polymer network is a process that affects the rate of polymer swelling significantly. The rate of relaxation of polymer chains in response to a stress depends on whether the polymer is above or below its glass transition temperature (T_g).[11] In rubbery systems above the T_g, relaxations are rapid and diffusion into the polymer network can occur, in agreement with Fick's laws.[5] Below the T_g, relaxation rates are finite due to time-dependent structural rearrangements.[5] These structural rearrangements can lead to deviations from Fickian behavior. Alfrey et al.[12] proposed three models that can be used to describe transport phenomena into glassy polymers based on the relative rates of penetrant diffusion and polymer chain relaxation:[13]

1. Case I (Fickian diffusion): The rate of penetrant diffusion is significantly slower than the rate of relaxation, and the mechanism is diffusion controlled.

2. Case II: The rate of penetrant diffusion is greater than the rate of polymer relaxation, and the mechanism is relaxation controlled.

3. Case III (anomalous): Complex diffusion behavior that lies between the extreme case I and case II models is observed. The rate of penetrant diffusion is comparable to the rate of polymer relaxation.

The water diffusion mechanism can be characterized by the profile of the sorption M_t/M_∞ versus time curves by using the following equation:[14]

$$\frac{M_t}{M_\infty} = kt^n \tag{1}$$

where M_t is the mass of water absorbed by the polymer at time t, M_∞ is the mass of water absorbed at equilibrium, k is a constant incorporating the characteristics of the macromolecular network system and the penetrant, and n is the diffusional exponent.

* To whom correspondence should be addressed. Address: The Centre for High Performance Polymers (CHPP), The Division of Chemical Engineering, The University of Queensland, Brisbane, Qld, 4072, Australia. Phone: +617 3365 4158. Fax: +61 7 3365 4199. E-mail: m.russo@uq.edu.au.

† The Centre for High Performance Polymers.

§ Centre for Magnetic Resonance.

‡ Australian Institute for Bioengineering and Nanotechnology.

10.1021/bm060791i CCC: $37.00
Published on Web 11/24/2006

The diffusional exponent, n, can be used as an indicator of the diffusion mechanism for a particular system. For a planar system, an exponent of 0.5 ($n = 0.5$) is indicative of Fickian diffusion, and $n = 1$ for case II diffusion and case III diffusion is shown by diffusional exponents between the limits of 0.5 and 1. Equation 1 is normally considered valid for up to the first 60% of normalized water uptake ($M_t/M_\infty \leq 0.60$).[3]

The work presented here is an investigation into the effect of moisture content and temperature on the water diffusion into a modified high amylose content TPS blend. Gravimetry and magnetic resonance imaging (MRI) were used to characterize water diffusion into this system. Gravimetric experiments allow monitoring of the macroscopic changes in polymer mass and swelling. MRI is a novel method used for studying water diffusion and swelling into polymers.[13,15−19] The technique is used to monitor microscopic changes in the water concentration throughout the cross-section of the polymer without any physical slicing of the polymer. A solvent front, also know as a water concentration profile, is the boundary that separates swollen and unpenetrated material throughout the cross-section of the polymer.[5] The diffusion coefficient can be calculated directly from the water concentration profile obtained by MRI images. MRI has been used previously to study water diffusion and swelling into other high amylose starch materials.[16,17,19,20] In these publications, the advance of the solvent front toward the center of the sample with time was used to calculate the rate constant for swelling. In this paper, the diffusion coefficients were calculated directly from the water concentration profiles obtained from the MRI images by comparing them to a theoretical profile calculated using the implicit Crank−Nicolson finite difference method. This method of determining diffusion coefficients is advantageous because the effect of concentration during the diffusion process can be investigated in detail.

Experimental Section

Preparation of Polymer. A modified high amylose maize TPS blend (≤90 wt % of starch) was supplied by Plantic Technologies Ltd. in the form of pellets. The starch was blended with a low amount of a water-soluble polyol (1−10%) in accordance with the patent.[21] These pellets were processed into films of 1.8 mm thickness using a compression moulder. The compression moulder was heated to 125 °C and to a force of 100 kN for 5 min. The compression moulder was then cooled to room temperature over approximately 10 min, and the pressure was released. After compression moulding, the film was cut into small rectangular samples of dimensions 1 × 0.5 × 0.18 cm and placed in desiccators maintained at 23, 43, 54, and 81% relative humidity for at least 2 weeks to allow for equilibration. Each relative humidity environment was achieved using appropriate salt solutions in the base of the desiccators. Separate samples were also placed in a vacuum oven for 4 days at 70 °C to remove moisture imbibed within the polymer.

Water Sorption Experiments. Once samples were equilibrated at each relative humidity and vacuum-dried environment, water sorption studies commenced in a water bath at three different temperatures: 25, 37, and 45 °C. The change in mass over time was measured in triplicate at predetermined time intervals by removing the samples from the reservoir of distilled water, removing excess surface water with a lint-free tissue, and determining the polymer mass with an analytical balance. The same three samples were used for each immersion time for each specific relative humidity and temperature condition studied. The change in dimensions was also monitored at these time intervals by using calipers. The change in polymer mass and the swelling was monitored over a 24 h period.

MRI. These experiments were carried out in parallel with the gravimetric experiments at each moisture content and temperature condition. Prior to imaging, the polymer samples were removed from the water bath, and excess surface water was removed using a lint-free tissue. The samples were then wrapped in Teflon tape to prevent water evaporation. Images were obtained using a Bruker AMX 300 spectrometer and acquired using the standard Bruker three-dimensional spin−echo pulse sequence (SE3D). The 90° pulse time was 12 μs, and the echo and repetition times were 6.8 ms and 3 s, respectively. The images consisted of 128 × 128 × 4 voxels. All the images have an in-plane resolution of 62.5 × 62.5 μm and a slice thickness of 0.2 mm in a field of view of 0.8 × 0.8 cm. The total acquisition time was approximately 25 min. It was confirmed that full relaxation of the magnetization occurred during the 3 s repetition time and also that the T_2 relaxation time of the water protons did not change substantially across the images. Therefore, the images provide an accurate representation of the relative water content throughout the polymer sample.

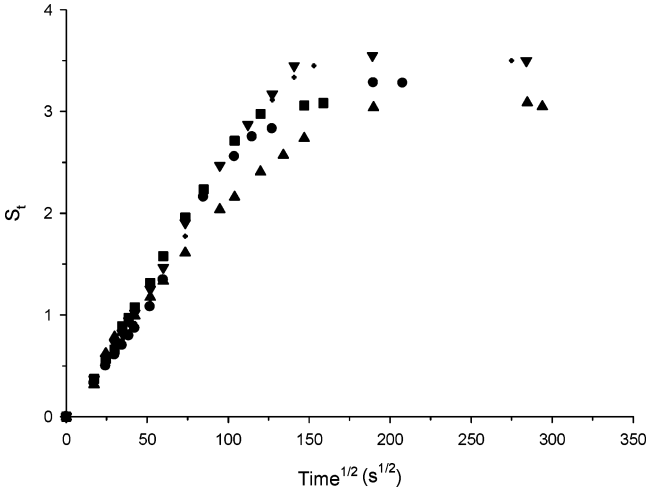

Figure 1. Sorption curves for the diffusion of water into a starch blend at 45 °C after conditioning at a range of relative humidity environments: ● vacuum-dried, • 23%, ▼ 43%, ■ 54%, ▲ 81% relative humidity.

Results and Discussion

Water Sorption Data. Figure 1 illustrates the fractional water uptake (S_t) into the starch blend films as a function of the square root of time for a series of samples held in water at 45 °C after equilibration at different relative humidities. The value of S_t is defined as the ratio of the absorbed mass of water at time t (M_t) to the initial mass of dry polymer (M_p).[13] This figure illustrates that the equilibrium water content was 300−350% for each moisture content condition, demonstrating that this starch blend can absorb 3−4 times its original mass.

$$S_t = M_t/M_p \tag{2}$$

Figure 2 illustrates the relationship between normalized water uptake (M_t/M_∞) and the square root of time for water diffusion into a starch blend conditioned at 23% relative humidity and studied at a water temperature of 45 °C. Similar curves were obtained for samples stored at other relative humidities and immersed in water at other temperatures. At short times, a linear relationship was obtained between normalized water uptake and the square root of time (up to $M_t/M_\infty \approx 0.40$). Thérien-Aubin et al. reported values of $M_t/M_\infty \approx 0.60$ for water diffusion into a cross-linked starch polymer blend for water temperatures between 25 and 45 °C.[19] Where $t^{1/2} \approx 50-60$, $s^{1/2}$, the slope of the line, increased, as indicated by the arrow in the diagram. In addition, an increase in the rate of swelling was observed at this point, as shown in Figure 3A.

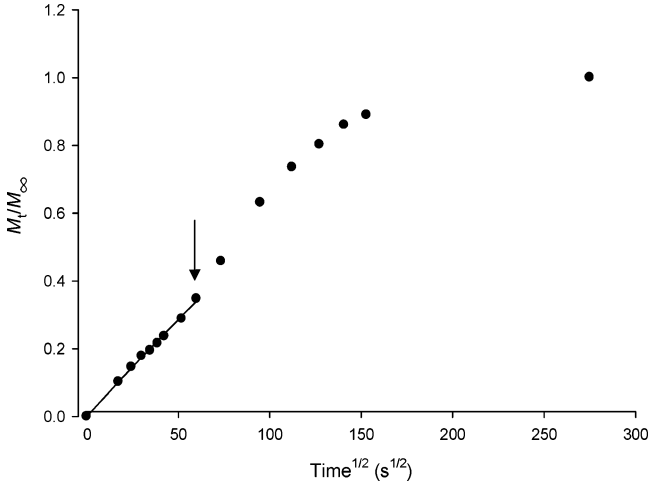

Figure 2. Normalized water uptake into a starch blend at a water temperature of 45 °C after being stored in a 23% relative humidity desiccator. The solid line denotes the best fit, where $D_0 = 2.4 \times 10^{-7}$ cm^2/s and $n = 0.5$ for a Fickian transport model. The arrow indicates the point where solvent fronts throughout the polymer cross-section meet. The rate of swelling after this point increases.

The change in the overall swelling of the polymer has been described as the swelling percent, defined as the increase in dimensions relative to the initial dimensions.[19]

The swelling data in Figure 3A was fitted to the following equation:[19]

$$S = S_{\max}(1 - e^{-kt}) \tag{3}$$

where S is the swelling at time t, $S_{\max}$ is the maximum swelling as time approaches ∞, and k is the rate of swelling.

In the starch blend studied here, anisotropic swelling was observed (where the swelling in thickness is larger than in the diameter dimension). Anisotropic was also observed by Thérien-Aubin et al. for water diffusion into a cross-linked high-amylase starch tablet.[19]

As will be demonstrated by the MRI results reported later, this was the point where the solvent fronts within the cross-section of the polymer meet. After this point, water sorption was significantly faster as the swelling of the rubbery sheath was no longer restricted by the central glassy core of the film.

As the immersion temperature increased toward the T_g of the material, the amount of water required to take the entire sample above the T_g decreased. This trend is summarized in Table 1, where the ratio of M_t/M_∞ decreased as the water temperature increased. These values of M_t/M_∞ were obtained by taking the average values over the five different relative humidity environments for each temperature condition studied. This behavior is consistent with the work of Gehrke et al. who observed a similar trend for the water transport into poly(hydroxyethyl methacrylate) at different temperatures.[11]

MRI Investigation of Water Diffusion. Determining the diffusion coefficient of a polymer−penetrant system by gravimetric studies involves continual monitoring of sorption changes over a period of time to be able to construct a sorption curve. Therefore, only an average diffusion coefficient can be determined for a specific condition and duration of gravimetric study. By using MRI to investigate the water distribution throughout the polymer, it is possible to visualize the solvent front throughout the polymer at any particular time during the sorption process. The solvent front obtained from the MRI images can be used to calculate the instantaneous diffusion coefficient at a particular time. This property alone of the MRI technique is very advantageous for water diffusion characterization, as it allows the dependence of the diffusion coefficient on the water content of the polymer to be studied.

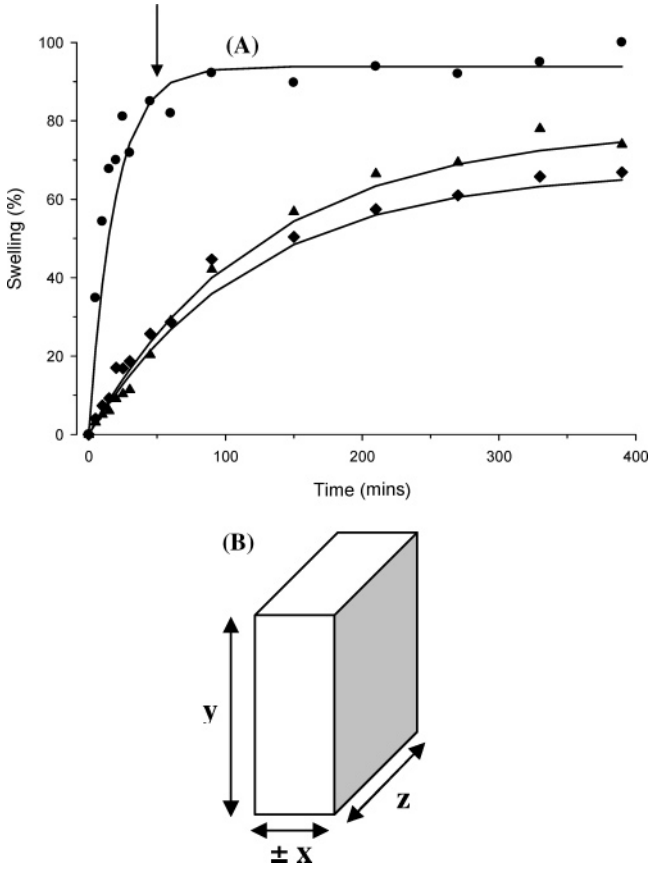

Figure 3. (A) Percentage of polymer swell for starch blend samples held in water at 45 °C after conditioning at 23% relative humidity: ● increase in x, ◆ increase in y, ▲ increase in z. The arrow indicates the point where solvent fronts have met throughout the cross-section of the sample. Solvent fronts meet, and the glassy core commences to disappear when $t \approx 45-60$ min. (B) Illustration of the directions of the polymer sample measured.

Table 1. Values of M_t/M_∞ for the Entire Sample to be above T_g at 25, 37, and 45 °C[a]

temperature (°C)	M_t/M_∞
25	0.63
37	0.49
45	0.25

[a] M_t/M_∞ values were averaged over the five relative humidity environments for each temperature condition.

Figure 4 shows a series of MRI images obtained over a 4 h period for a starch blend material conditioned at 23% relative humidity and immersed in water at 45 °C. The intensity in these images denotes the water concentration. As the immersion time is increased, a higher water concentration is observed throughout the cross-section. For Figure 4A, the center of the polymer is still in a glasslike state, as shown by the lack of water protons throughout the cross-section. Figure 4B illustrates some degree of water intensity throughout the polymer center, indicating that the solvent fronts have met. In Figure 4C,D, the entire polymer sample is above its T_g, as the water concentration is the same throughout the polymer cross-section. The amount of polymer swell over time is evident in these series of images.

Figure 5 illustrates a series of MRI images obtained over a 4 h period for a starch blend material conditioned at 23% relative humidity and immersed in water at 25 °C. It is evident by

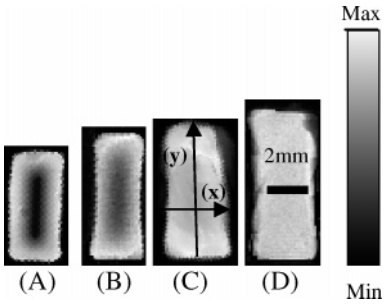

Figure 4. MRI images showing the intensity of water protons across the diameter of a starch blend film initially conditioned at 23% relative humidity and in water at 45 °C after (A) 30 min, (B) 1 h, (C) 2 h, (D) 4 h. In image C, *x* indicates the thickness direction and *y* indicates the width direction.

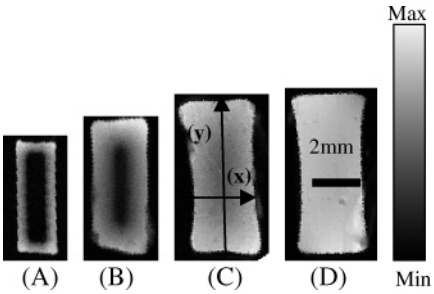

Figure 5. MRI images showing the intensity of water protons across the diameter of a starch blend film initially conditioned at 23% relative humidity and in water at 25 °C after (A) 30 min, (B) 1 h, (C) 2 h, (D) 4 h. In image C, *x* indicates the thickness direction and *y* indicates the width direction.

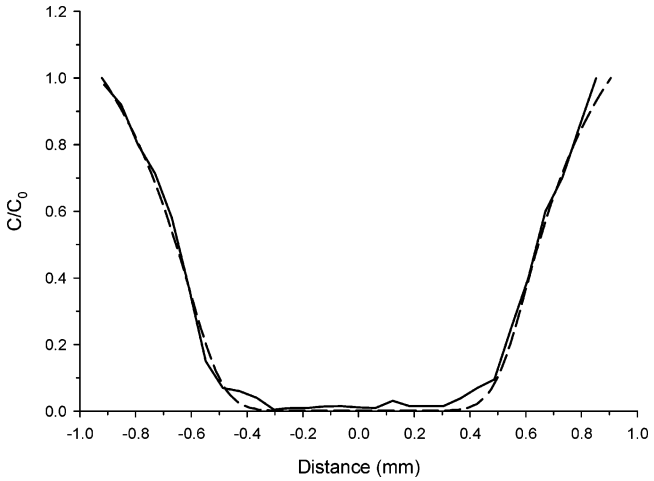

Figure 6. Experimental water concentration profile (—) compared to the theoretical fit (– – –) along the *x*-axis of a starch film conditioned at 43% relative humidity and immersed in water at 37 °C for 10 min.

comparing the MRI images summarized in Figures 4 and 5 that there is a higher concentration of water present within the polymer studied at a higher water temperature (45 °C) compared to the samples studied at a lower water temperature (25 °C) summarized in Figure 5, where the duration of immersion in water was kept constant.

Figure 6 shows the water concentration profile derived from the cross-section of an MRI image for a starch blend sample initially dried in a vacuum oven, then immersed in water at 25 °C for 10 min. This experimental profile is compared to a calculated concentration-dependent Fickian diffusion model that takes into account the polymer swell. It was found that the theoretical concentration-dependent Fickian model described the water diffusion best in this starch blend. This is reflected by the convex water concentration profile shape within the polymer studied here, reported by George et al. as a characteristic trait for concentration-dependent Fickian diffusion.[13] Concave profiles depict concentration-independent Fickian diffusion.

Determination of Diffusion Mechanism and Coefficient. The solvent front through the cross-section of the polymer sample can be obtained directly from the MRI data, and, from a single image, the diffusion coefficient can be determined at that particular time.

In the study, diffusion coefficients were calculated by comparing the experimental MRI data to a theoretical model generated by solving the one-dimensional Fickian diffusion model:[22]

$$\frac{\partial C}{\partial t} = D\frac{\partial^2 C}{\partial x^2} \tag{4}$$

In our study, the best fit to the experimental data could only be made by applying an exponential dependence on the concentration. Therefore, the diffusion coefficient (D) was assumed to be exponentially dependent upon the concentration:

$$D = D_0 e^{A(C/C_0)} \tag{5}$$

where C is the concentration at a point, C_0 is the concentration at the surface, and D_0 and A are constants.

During water sorption, this system swelled appreciably, and this swelling was taken into consideration by modifying the diffusion rate and rescaling the linear distances. The diffusion rate becomes

$$D_1 = D_0 \frac{e^{A(C/C_0)}}{1 + S_\infty(C/C_0)} \tag{6}$$

where S_∞ is the degree of swelling calculated as the maximum thickness of the sample at full swelling thickness divided by the initial thickness of the polymer.

For diffusion in a plane sheet when the diffusion coefficient, D, is constant, convenient variables are

$$X = \frac{x}{l},\ T = \frac{D_0 t}{l^2},\ c = \frac{C}{C_0},\ D = \frac{D_1}{D_0}$$

where l is the half thickness of the polymer sample.

In this particular case, the diffusion coefficient is concentration dependent, and it is useful to introduce the variable:

$$s = \int_0^c D\mathrm{d}c / \int_0^1 D\mathrm{d}c \tag{7}$$

In terms of s, eq 7 may be written as

$$\frac{\partial s}{\partial t} = D\frac{\partial^2 s}{\partial x^2} \tag{8}$$

Equations 4 and 8 were solved using the implicit Crank–Nicolson finite difference method, where the nondimensional step change for distance was $\delta X = 0.02$, and, for time, $\delta T = (\delta X)^2/2$. Symmetry about the center of the sample was assumed.

The real values of concentration as a function of time and distance were obtained by reversing the transformations. The

Table 2. Summary of Values of D_0, A, and n Determined from the Analysis of the MRI Images at 25, 37, and 45 °C

	25 °C			37 °C			45 °C		
condition	$D_0 \times 10^{-7}$ (cm^2/s)	A	n	$D_0 \times 10^{-7}$ (cm^2/s)	A	n	$D_0 \times 10^{-7}$ (cm^2/s)	A	n
vac dried	0.6 ± 0.6	2.2 ± 0.1	0.50	1.2 ± 0.4	2.3 ± 0.1	0.50	2.3 ± 0.3	2.2 ± 0.2	0.53
23%	1.3 ± 0.7	2.3 ± 0.1	0.53	1.8 ± 0.5	2.3 ± 0.1	0.57	2.4 ± 0.5	2.3 ± 0.1	0.50
43%	1.6 ± 0.1	2.1 ± 0.3	0.51	2.0 ± 0.2	2.2 ± 0.1	0.52	2.5 ± 0.7	2.2 ± 0.2	0.50
54%	1.8 ± 0.6	2.3 ± 0.2	0.50	2.7 ± 0.6	2.1 ± 0.5	0.51	2.9 ± 0.1	1.6 ± 0.2	0.52
81%	2.4 ± 0.1	2.2 ± 0.2	0.47	3.3 ± 0.4	2.2 ± 0.2	0.50	3.8 ± 0.4	2.2 ± 0.1	0.50

swelling is accounted for by applying the following transformation for distances:

$$x_j = l\mathrm{d}X \sum_{i=0}^{j}(1 + S_\infty c_i) \tag{9}$$

The MRI images were measured and analyzed over the range of $0.10 \leq M_t/M_\infty \leq 1.0$. It was observed that, once the glassy core disappeared, there was an abrupt change in the dimensions of the polymer. Therefore, at this point, the diffusion kinetics change, and the concentration-dependent Fickian diffusion model would no longer describe this system. This was also observed by George et al. in their concentration-dependence study for water diffusion into HEMA-MOEP hydrogels.[13]

The values of D_0 and A summarized in Table 2 were calculated from profiles with values of $M_t/M_\infty \leq 0.60$. Values of n were determined from the gravimetric data under the same M_t/M_∞ restriction. The errors in D_0 and A were determined by calculating the standard deviation in the data. There is a general trend for D_0 to increase with temperature and storage relative humidity. Diffusion is faster at higher temperatures due to the increase in kinetic energy of the water molecules and faster relaxation of the polymer. Faster diffusion for samples conditioned at higher relative humidity conditions can be explained by an increase in free volume due to plasticization with water molecules at higher relative humidities. The average D_0 value calculated for each relative humidity storage condition increased as the relative humidity storage environment increased, although the standard deviation in the data suggests that this increase is not significant. It is a plausible result that the water diffusion increased with higher relative humidity storage environments, as there would be more plasticization due to the higher concentration of sorbed vapor. The plasticization due to the higher concentration of sorbed vapor facilitates diffusion by increasing polymer chain flexibility and mobility. The values of n indicate that water diffusion follows the Fickian diffusion mechanism.

The possibility of dissolution of the polymer during the water sorption studies was considered, and it was found that there was no significant loss of mass of polymer up to the first 2 h of water diffusion into the material (less than 10 wt % of polymer).

As previously mentioned by George et al.[13] Crank considered in great detail the effect of a concentration-dependent diffusion coefficient when analyzing the swelling of polymers. As reported earlier, the best fit to the experimental data could only be made by using an exponential dependence of D on the concentration. George et al. also gave reference to Erying's "hole theory of diffusion", which can be used to explain this behavior.[13] This theory was first popularized by Barrer[23] and can be used to describe diffusion in amorphous polymers. The hole theory of diffusion in amorphous materials is an extension of the lattice vacancy or defect theories of diffusion in crystals. According to this theory, there are, in any liquid or solid, a number of holes arising from thermal fluctuations; diffusion takes place by a molecule leaving its current position and jumping into a near-neighbor hole. These holes are created by Brownian or segmental movement of the molecular chain segments and by a number of van der Waals bonds breaking, giving rise to a site of higher energy; the amount of energy required increases with the size of the hole. Thus, according to Boltzmann's law, the concentration of holes decreases exponentially with their size. Assuming that the polymer−penetrant bonds are weaker than polymer−polymer bonds, then the energy required for a hole of a certain size decreases linearly with increasing penetrant concentration. If the number of holes is big enough to permit, diffusion should increase exponentially with increasing penetrant concentration. The diffusion coefficient is approximately proportional to the number of holes per unit volume, and the diffusion coefficient should increase in an exponential manner with concentration.

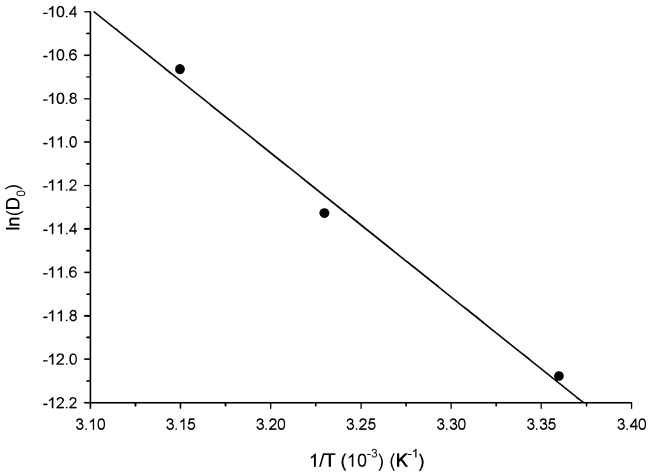

Figure 7. Arrhenius plot of the starch blend after storage in the vacuum oven. The experimental E_a values are shown by circles, and the solid line is the fit to the Arrhenius equation.

Activation Energies (E_a). The values of D_0 increase significantly with increasing temperature, which allows the calculation of the activation energy for each moisture content condition studied. The values of D_0 determined from the MRI images were used to construct an Arrhenius plot of the logarithm of D_0 ($\ln D_0$) versus the inverse of temperature ($1/T$). Figure 7 shows an Arrhenius plot for starch blend samples stored in the vacuum oven. Similar plots were constructed for the remaining four relative humidities.

Table 3 summarizes the values of the E_a calculated for each moisture content condition. The error was determined by comparing E_a values calculated using the mean values of D_0 to the E_a values calculated using values of $D_0 \pm 1$ standard deviation. The E_a results obtained in this study are realistic, as they compare to the E_a values obtained by Thérien-Aubin et al. for water diffusion into a chemically modified high amylose

Table 3. Summary of E_a Values Calculated for Each Relative Humidity Storage Condition

condition	E_a (kJ/mol)
vac dried	55 ± 18
23%	23 ± 9
43%	18 ± 6
54%	21 ± 10
81%	18 ± 3

starch tablet.[19] Thérien-Aubin et al. report E_a's in the range of 26−42 kJ/mol. E_a values in the range of 20−40 kJ/mol are consistent with the potential energy of hydrogen bonds.[19] Therefore, the E_a values obtained for the starch blend conditioned at 23−81% relative humidity are consistent with the range of the potential energy of hydrogen bonds. The E_a for the vacuum-dried samples was significantly higher than the E_a's for the remaining relative humidity conditions studied. Water diffusion into vacuum-dried samples requires more energy to diffuse into the material, as there is limited chain flexibility and plasticization within this dry polymer. Although, in this case, the error is somewhat significant, and a definite conclusion cannot be drawn. Overall, it was observed that the values of E_a decrease with an increase in moisture content due to more plasticization and chain flexibility within the polymer.

Conclusions

Water diffusion into this high amylose starch blend was significantly affected by the water temperature during the sorption study and generally by the relative humidity storage conditions of the material. Diffusion was faster into samples studied at higher water temperatures due to an increase in kinetic energy of the water molecules and free volume within the polymer. At higher relative humidity environments, there was an increase in free volume and plasticization within polymer samples, facilitating water diffusion into the material, although the standard deviation in the data suggests this increase may be insignificant. MRI has been a very useful technique for providing information on the mechanism of water diffusion into this starch blend material. This imaging technique allowed the effect of concentration dependence on the mechanism of water diffusion to be studied. At the time of writing this paper, there were no other papers present in the literature on the study of concentration dependence on the water diffusion into starch blends in this detail. These starch blend materials exhibited anisotropic swelling (a larger swelling in thickness than in diameter) (Figure 3A), also reported by Thérien-Aubin and coworkers in their water diffusion work on chemically modified starch-based tablets.[19] To deduce more information about the water diffusion process observed here, water diffusion into the individual blend components should be studied.

Acknowledgment. We would like to thank Prof. Andrew Whittaker for helpful discussions about this work and Dr. Martin Markotsis for assisting in the preliminary scope of the study. The financial support of Plantic Technologies Ltd. and the Australian Research Council is acknowledged with thanks.

References and Notes

(1) Averous, L. *J. Macromol. Sci., Part C: Polym. Rev.* **2004**, *44*, 231−274.
(2) Averous, L.; Moro, L.; Dole, P.; Fringant, C. *Polymer* **2000**, *41*, 4157−4167.
(3) Peppas, N. A.; Brannon-Peppas, L. *J. Food Eng.* **1994**, *22*, 189−210.
(4) Gopferich, A. In *Handbook of Biodegradable Polymers*; Domb, A. J., Kost, J., Wiseman, D. M., Eds.; Harwood Academic Publishers: Amsterdam, 1997.
(5) Thomas, N. L.; Windle, A. H. *Polymer* **1981**, *22*, 627−639.
(6) Treloar, L. R. *The Physics of Rubber Elasticitiy*, 3rd ed.; Clarendon: Oxford, 1975.
(7) Flory, P. J. *Principles of Polymer Chemistry*; Cornell Univeristy Press: New York, 1953.
(8) Smith, K. J. In *Theories of Chain Coiling, Elasticity and Viscoelasticity*; Jenkins, A. D., Ed.; North Holland: Amsterdam, 1973; Vol. 1.
(9) Dreschel, P.; Hoard, J. L.; Long, F. A. *J. Polym. Sci., Part B: Polym. Phys.* **1953**, *10*, 241.
(10) Park, G. S. *J. Polym. Sci.* **1953**, *11*, 97.
(11) Gehrke, S. H.; Biren, D.; Hopkins, J. J. *J. Biomater. Sci., Polym. Ed.* **1994**, *6*, 375−390.
(12) Alfrey, J. T.; Gurnee, E. F.; Lloyd, W. G. *J. Polym. Sci., Part C: Polym. Symp.* **1966**, *12*, 249−261.
(13) George, K. A.; Wentrup-Byrne, E.; Hill, D. J. T.; Whittaker, A. K. *Biomacromolecules* **2004**, *5*, 1194−1199.
(14) Frisch, H. L. *Polym. Eng. Sci.* **1980**, *20*, 2−13.
(15) Ghi, P. Y.; Hill, D. J.; Whittaker, A. K. *Biomacromolecules* **2001**, *2*, 504−510.
(16) Baille, W. E.; Malveau, C.; Zhu, X. X.; Marchessault, R. H. *Biomacromolecules* **2002**, *3*, 214−218.
(17) Malveau, C.; Baille, W. E.; Zhu, X. X.; Marchessault, R. H. *Biomacromolecules* **2002**, *3*, 1249−1254.
(18) Hill, D. J. T.; Chowdhury, M.; Ghi, P. Y.; Moss, N. G.; Whittaker, A. K. *Macromol. Symp.* **2004**, *207*, 111−123.
(19) Therien-Aubin, H.; Baille, W. E.; Zhu, X. X.; Marchessault, R. H. *Biomacromolecules* **2005**, *6*, 3367−3372.
(20) Hopkinson, I.; Jones, R. A. L.; Black, S.; Lane, D. M.; McDonald, P. J. *Carbohydr. Polym.* **1997**, *34*, 39−47.
(21) Buehler, F. S. E; Schultze, H. J. EMS-Inventa AG. US Patent, 1994.
(22) Crank, J.; Park, G. S. *Diffusion in Polymers*; Academic Press: London/New York, 1968.
(23) Barrer, R. M. *Diffusion In and Through Solids*; The University Press: Cambridge, UK, 1941.

BM060791I